CHEMICAL ENGINEERING TRANSACTIONS
VOL. 108, 2024

A publication of AIDIC
The Italian Association of Chemical Engineering
Online at www.cetjournal.it

Guest Editors: Carlo Pirola, Antonio Espuña

ISBN 979-12-81206-08-3; **ISSN** 2283-9216

DOI: 10.3303/CET24108006

Effect of Magnetic Field on CO_2 Injection for Carbonate Dissociation without Catalyst and Additives

Ahmad F. K Wijaya, Muhammad D. Bustan*, Sri Haryati

Universitas Sriwijaya, Palembang, Indonesia
muhammaddjonibustan@ft.unsri.ac.id

Unutilized CO_2 can be utilized to decompose carbonates at low temperatures through the magnetic field effect so that it can reduce air CO_2 gas emissions. This study identifies the optimal parameters required in the carbonate dissociation reaction by considering volume, temperature, electric current, and pressure. Tests were conducted by monitoring hourly pressure and weight changes before and after CO_2 injection. The results showed that the optimal carbonate dissociation parameters were volume 50 ml, weight 50.01 g, electric current 15 A, and temperature 90°C with an inlet pressure of 30 psi. Utilization of a magnetic field with a strength of 9 - 10 T resulted in a weight reduction of 8.3 g. The carbonate dissociation reaction under the influence of the magnetic field degraded the elemental levels of C (8%) and O (4%) and increased the elemental level of Ca (31%). CO_2 can effectively induce carbonate dissociation when in a magnetic field.

1. Introduction

Oil well mining areas significantly affect the surrounding environmental ecosystem (Cherepovitsyn and Ilinova, 2016). Besides wanting to get natural resources in the form of oil and gas, the mining process causes various natural damages, such as damage to the soil of the mining area (Rabczak and Proszak-Miąsik, 2016; Sinharoy et al., 2020; Useche-Narvaez et al., 2022). Apart from soil damage, air ecosystems are also affected by this mining process, such as CO_2 gas produced from reservoirs (Köne and Büke, 2010). Currently, CO_2 gas produced from the gas refining process is often not optimally utilized in various reservoirs. This CO_2 gas is often released into the atmosphere in the form of CO_2 impurities after the refining process. This will be dangerous if the CO_2 gas content in the air is excessive. Because of its greenhouse effect, CO_2 contributes to global warming (Anwar et al., 2019; Lashof and Ahuja, 1990; Litvak and Litvak, 2020; West and Marland, 2002).

One way to overcome CO_2 gas emissions in the air is to utilize it as a single initiator in the decomposition process of carbonate rocks. So far, the decomposition of carbonate rocks has used catalysts, additives, or thermal decomposition, which takes place at high temperatures in the reaction process. As done by Cui et al., thermal decomposition of carbonate with a calciner at a temperature of 1073 K and a pressure of 100,445 Pa (Cui et al., 2023). Song et al. decomposed carbonate with doped Al and Fe metals with operating temperatures reaching 700 °C (Song et al., 2021). Carbonate rocks, before being decomposed at 1000 °C, were deposited in ammonia and alkylamine solutions by Popescu et al. (2014). These studies show that the carbonate decomposition process still uses high temperatures, even with various chemical compound preparations or directly with heat. CO_2 can be a solution for processes that take place at low temperatures.

CO_2 can generate a magnetic field because it is an ionic compound. CO_2 can generate a magnetic field because it is a charged molecule. This magnetic field can affect chemical reactions in the system when charged species move at a certain speed, and this phenomenon is referred to as the Lorentz force (Crnogorac et al., 2020; Kolawole et al., 2020; Syed et al., 2022). Processes using magnetic fields do not need to use high operating temperatures because the electron transfer in decomposing carbonate rocks can match the thermal decomposition process at high temperatures. There have been many reactions that use magnetic field effects that can take place under low-temperature conditions. Chernavsky et al. studied the effect of magnetic fields on the reduction of magnetite with hydrogen, with the operating temperature used being 350 °C and the general operating temperature being T>450 °C (Chernavsky et al., 2021). Gupta et al. research on evolving hydrogen

Paper Received: 20 November 2023 ; Revised: 21 December 2023 ; Accepted: 20 January 2024
Please cite this article as: Wijaya A.F.K., Bustan M.D., Haryati S., 2024, Effect of Magnetic Field on CO_2 Injection for Carbonate Dissociation Without Catalyst and Additives, Chemical Engineering Transactions, 108, 31-36 DOI:10.3303/CET24108006

shows that its evolutionary activity increases at room operating temperature in a magnetic field (Gupta et al., 2020). Apart from temperature, the magnetic field effect also provides advantages in some reactions. For example, in a study of the electrochemical polymerization of polyaniline under the influence of a magnetic field (Wang and Yang, 1995), the MFE effect was seen in the aniline-free radical polymerization process. When a magnetic field was applied, it showed increased polymerization rate, molecular weight, conductivity, and solubility (Hu et al., 2011). MFE can also reveal unusual phenomena and complex mechanisms in magnetized charge transfer electrochemical systems within the reaction zone (Al-Douri et al., 2022). In addition, the MFE effect has been shown to improve the photocatalytic degradation efficiency of benzene during photocatalysis (Hu et al., 2014). The study of the effect of MFE on chemical reactions involves understanding various aspects, including reaction pathways, growth behaviour of nanomaterials, product phases, and magnetic domains in the materials concerned (Hu et al., 2019). From these aspects, this research will study the process of carbonate rock decomposition by utilizing the magnetic field effect produced by CO_2 gas without catalysts and other additives in the hope that it can occur under low-temperature operating conditions.

2. Methods and Materials

2.1 Materials

Pure calcium carbonate ($CaCO_3$) from Pertamina, Indonesia and CO_2 gas from Pertamina, Indonesia.

2.2 Magnetic field measurement when CO_2 is flowing

The magnetic field was measured at intervals of every 10 cm in a tube under stationary flow conditions. Then, CO_2 gas flowed for 30 minutes until it reached a steady flow rate. After reaching this condition, the magnetic field was measured at tube intervals of every 10 cm when the CO_2 gas flow was set at levels 1, 2, 3, 10, 20, 30, 40, 50, and 60 Nl/min. This process determines the flow value that gives optimal magnetic field results.
A rectifier panel was prepared, and it was confirmed that it could be set to produce three levels of current output, namely 5A, 10A, and 15A. A 5mm cable was also prepared to transmit the voltage to the magnetic field. Tests were conducted using the test parameters that gave the best results. These parameters included hourly pressure and weight changes before and after CO_2 flow. In addition, the contact time between CO_2 and $CaCO_3$ rock and the magnetic Gibbs free energy (ΔGM) analysis were analyzed to determine the most optimal parameters in the $CaCO_3$ dissociation reaction process into CaO and CO_2.

2.3 Materials Characterization

Pure calcium carbonate was tested using X-ray Diffraction (XRD) and Energy Dispersive X-ray Spectroscopy (EDX) techniques, while CO_2 gas was measured and its composition analyzed using a Gas Chromatograph (GC).

3. Results and discussion

3.1 Quantitative calculation of Gibbs free enthalpy generated by magnetic field ΔGM and Gibbs thermal free energy ΔGT(T)

The dissociation process of $CaCO_3$ into CaO and CO_2 cannot occur at room temperature because the Gibbs energy of the products is higher than that of the reactants. Therefore, external energy is required to allow the dissociation reaction to occur. This experiment will calculate the Gibbs energy value at 90 °C and the magnetic energy applied to the reactor tube during the testing process. The equation used in this experiment is as follows:

$$\Delta H_{reaction} = \Delta H_f\,(Product) - \Delta H_f\,(Reactant) \quad (1)$$

$$\Delta S_{reaction} = \Delta S\,(Product) - \Delta S\,(Reactant) \quad (2)$$

$$\Delta GT = \Delta H - T\Delta S \quad (3)$$

$$\Delta GM = -(1/2)\mu 0(\chi\gamma - \chi\alpha)\, H^2 \quad (4)$$

The change in temperature during the dissociation process causes the Gibbs energy required for the reaction to drop from 323 kJ/mol to 264.7385 kJ/mol. In addition, applying a magnetic field to the reactor tube during the experimental process positively impacted the formation of CaO and CO_2. This shows that the presence of a magnetic field tends to support the dissociation process. The dissociation process is also assisted by mechanical energy generated through molecular collisions between the CO_2 stream and the $CaCO_3$ material contained in the reactor tube.

3.2 Magnetic field measurement when CO_2 is flowing

Based on the experimental results of CO_2 gas flowing for 30 minutes with different flow rate variations, the data shows that in the measurement range between 120 to 180 cm, there is an increase in the average magnetic field of 0.115 T. In comparison with the basic magnetic field without flow (red line), which has an average magnetic field of 0.045 T, this phenomenon indicates that the change in CO_2 flow when approaching the elbow of the reactor tube is one of the factors that may cause an increase in the magnetic field in the 120-180 cm range. This is also the basis for placing the $CaCO_3$ sample in this study.
Therefore, $CaCO_3$ samples with a certain amount and volume will be placed inside the reactor tube in the 120-180 cm range. In this experiment, a flow rate of 30 Nl/min is used because test results show that this flow rate produces a more stable magnetic field than other flow rates. In addition, at each point in the reactor tube, the magnetic field is higher than the base magnetic field, indicating that an increase in the magnetic field affected by CO_2 flow occurs at each point in the reactor tube, with the most significant increase occurring in the 120-180 cm range.

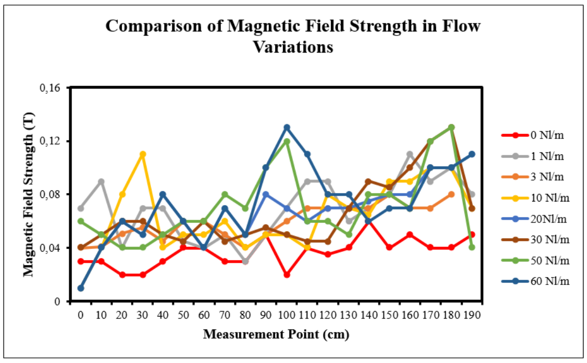

Figure 1. Measurement of the magnetic field when CO_2 gas flows with various flow variations

Based on the experimental results of CO_2 gas flowing for 30 minutes with different flow rate variations, the data shows that in the measurement range between 120 to 180 cm, there is an increase in the average magnetic field of 0.115 T. In comparison with the basic magnetic field without flow (red line), which has an average magnetic field of 0.045 T, this phenomenon indicates that the change in CO_2 flow when approaching the elbow of the reactor tube is one of the factors that may cause an increase in the magnetic field in the 120-180 cm range. This is also the basis for placing the $CaCO_3$ sample in this study.
Therefore, $CaCO_3$ samples with a certain amount and volume will be placed inside the reactor tube in the 120-180 cm range. In this experiment, a flow rate of 30 Nl/min is used because test results show that this flow rate produces a more stable magnetic field than other flow rates. In addition, at each point in the reactor tube, the magnetic field is higher than the base magnetic field, indicating that an increase in the magnetic field affected by CO_2 flow occurs at each point in the reactor tube, with the most significant increase occurring in the 120-180 cm range.

3.3 Obtaining Optimum Pressure, Current and Temperature Test Parameters in the Process of Decomposing $CaCO_3$ into CaO and CO_2

This experiment tested various test parameters by keeping the flow rate fixed at 30 Nl/min. The pressure parameters were tested in the ranges of 10 psig, 14 psig, and 30 psig, with the minimum volume, weight, current strength, and temperature set at 30 ml, 28.2407 g, 70 ˚C, and 5 A. The one-hour experiment showed that using a pressure of 30 psi (Figure 2) can increase pressure, which is indicative of the $CaCO_3$ decomposition reaction. Another test parameter search was to determine the current strength to be used in the experiment. Determination of the flow pressure parameters was tested with various levels of current strength, namely 5, 10 and 15 A, with the following volume, weight and temperature: 50 ml volume, 49.9834 g weight, 80 °C temperature, and 70 ml volume, 70.0004 g weight, 90 °C temperature.
The results of the experiments conducted for one hour show that using a current strength of 15 A (Figure 3) impacts increasing the pressure, which can indicate that the $CaCO_3$ decomposition reaction occurs.

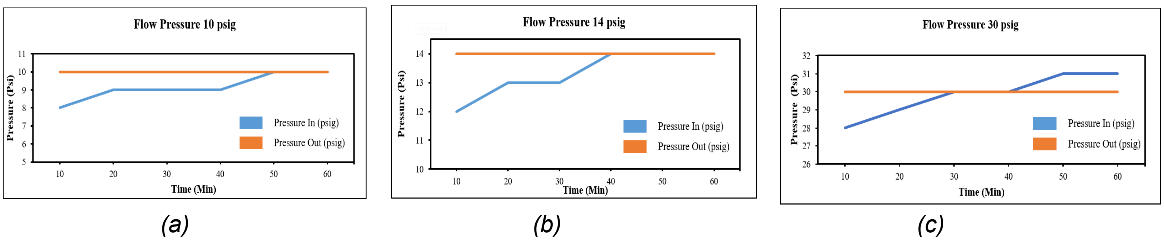

Figure 2. Test results with flow pressure test parameters: (a) 10 psig; (b) 14 psig; and (c) 30 psig

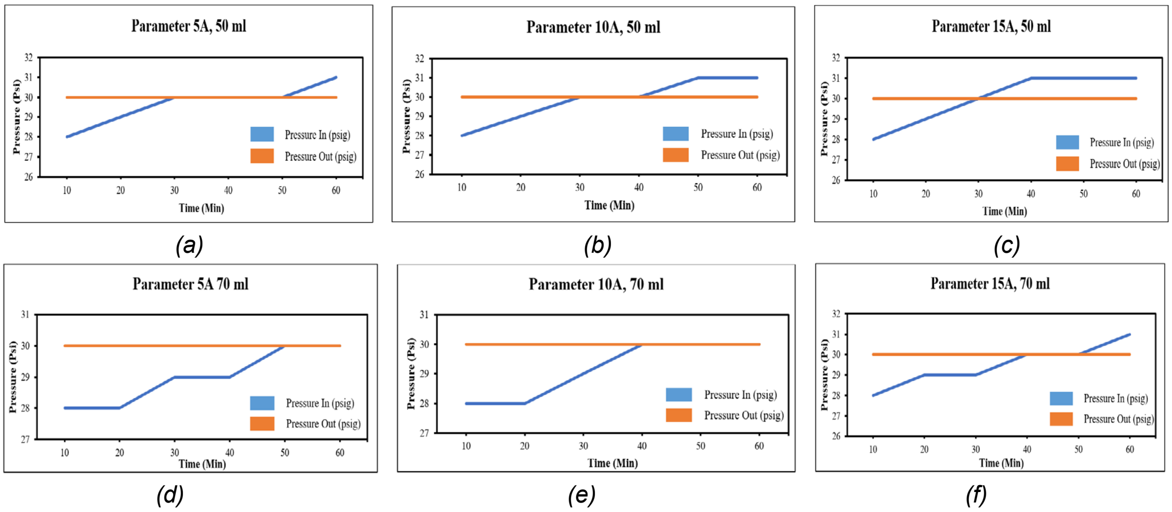

Figure 3. Test results with test parameters of current strength at 50 ml: (a) 5 A; (b) 10 A and (c) 15 A and current strength at 70 ml: (d) 5 A; (e) 10 A and (f) 15 A.

The test parameters that will be determined next are the volume and temperature parameters that will be applied to the trial in determining the flow pressure parameters tested with a volume range of 30 ml, 50 ml, and 70 ml while for temperatures of 80 ˚C and 90 ˚C and current strength parameters and optimal flow pressure that have been obtained previously. Based on the experiments carried out for one hour, it was found that a volume of 50 ml and a temperature of 90 ˚C (Figure 4) can affect the addition of pressure, indicating the decomposition of $CaCO_3$.

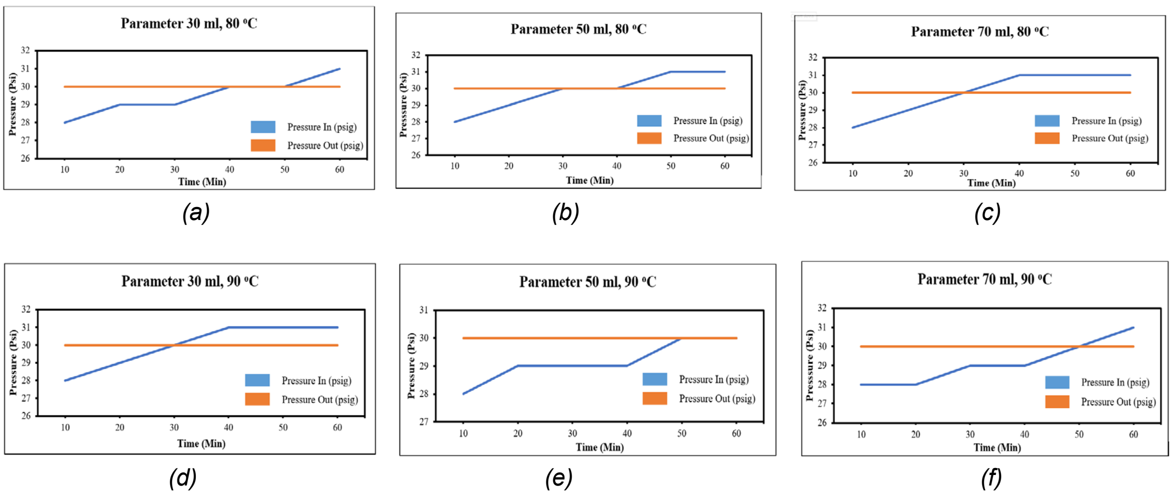

Figure 4. Test Results with 80 °C temperature range test parameters: (a) 30 ml; (b) 50 ml and (c) 70 ml and 90 °C temperature: (d) 30 ml; (e) 50 ml and (f) 70ml

3.4 Extended Flow testing on Tube Reactor using CaCO3 rock

Further experiments were conducted based on the previously identified optimal parameters. The magnetic field was applied prior to extended flow by keeping the magnetic field in line with the magnetic field readings, as shown in Figure 5. The $CaCO_3$ rock used came from drill cuttings with a volume of 50 ml, weight of 50.0129 g, temperature of 90˚C, current strength of 15 A, and an input pressure of 30 psi. Experimental nine-hour results indicated a weight change of 8.3288 g (Figure 6).

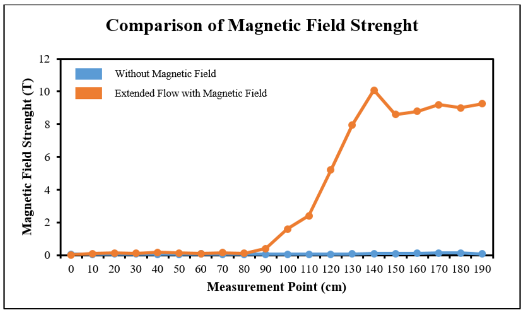

Figure 5. Comparison of Magnetic Field Strength

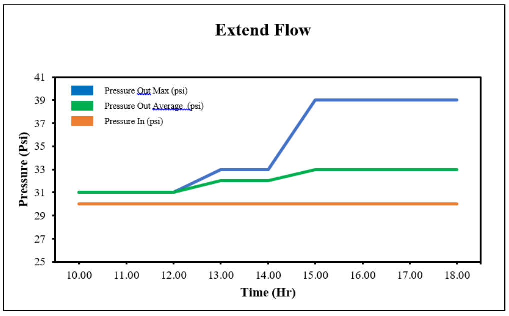

Figure 6. Extended flow at 50 ml vol, 50.0129 g, temperature 90˚ C, strong current 15 A, inlet pressure 30 psi.

Through EDX analysis of the carbonate rock that has been inserted into the reactor tube, data on its main composition was obtained, namely Oxygen (O) by 58.4%, Carbon (C) by 22.4%, and Calcium (Ca) by 18.9% (Figure 7). This analysis shows a decrease in C content by 8% and O by 4%, while Ca content increased by 31% when compared to the overall rock composition. This may indicate the dissociation of CO_2 from $CaCO_3$.

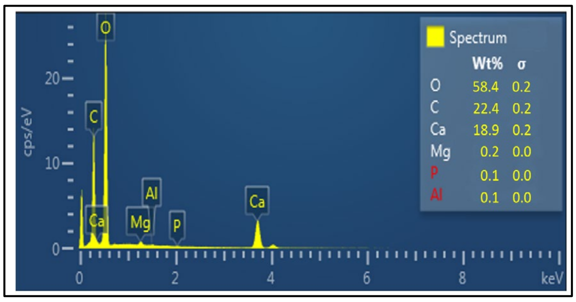

Figure 7. EDX analysis of carbonate rock after reaction

4. Conclusions

A magnetic field, molecular collisions, and temperature in the reaction process enable the dissociation between $CaCO_3$ and CO_2. This can be observed through temperature calculations, which reduce the Gibbs energy required from 323 KJ/mol to 264.7385 KJ/mol. The introduction of a magnetic field providing 7.0435 J/mol in Gibbs energy further enhances the likelihood of this dissociation process. Additionally, molecular collisions between CO_2 and $CaCO_3$ rocks also support the possibility of this dissociation process. In the experiment with 50 ml volume, 50.0129 g weight, a temperature of 90°C, 15 amperes of current, 30 psi inlet pressure, and an initial magnetic field of 9-10 T, conducted for nine hours, a weight reduction of 8.3288 g was observed in $CaCO_3$ drilling cuttings. Moreover, the EDX analysis of the carbonate rock from drilling indicates an 8% reduction in C, a 4% reduction in O, and a 31% increase in Ca based on the overall rock composition. This suggests the occurrence of a CO_2 dissociation process from $CaCO_3$. CO_2 produced in carbonate rocks can theoretically potentially increase the reservoir recovery factor and increase reservoir pressure from the production of CO_3 gas dissociated from carbonate rocks.

References

Al-Douri, Y., Hassan, S.M., Bouhemadou, A., El-Rehim, A.F.A., 2022. Magnetic field effect on nanoscaled water: Structural and optical investigations. Journal of Physics and Chemistry of Solids 171, 110981.

Anwar, M.N., Iftikhar, M., Khush Bakhat, B., Sohail, N.F., Baqar, M., Yasir, A., Nizami, A.S., 2019. Sources of Carbon Dioxide and Environmental Issues. pp. 13–36.

Cherepovitsyn, A., Ilinova, A., 2016. Ecological, Economic And Social Issues Of Implementing Carbon Dioxide Sequestration Technologies In The Oil And Gas Industry In Russia. Journal of Ecological Engineering 17, 19–23.

Chernavsky, P.A., Kim, N. V., Andrianov, V.A., Perfiliev, Y.D., Novakova, A.A., Perov, N.S., 2021. The influence of an external magnetic field on the dynamics of magnetite reduction with hydrogen. RSC Advances 11, 15422–15427.

Crnogorac, M., Tanasijević, M., Danilović, D., Karović Maričić, V., Leković, B., 2020. Selection of Artificial Lift Methods: A Brief Review and New Model Based on Fuzzy Logic. Energies 13, 1758.

Cui, Y., Yu, C., Shi, D., Wang, X., 2023. Simulation on coal combustion and calcium carbonate decomposition in a 5500 t/d full scale cement calciner. Applied Thermal Engineering 235, 121299.

Gupta, U., Rajamathi, C.R., Kumar, N., Li, G., Sun, Y., Shekhar, C., Felser, C., Rao, C.N.R., 2020. Effect of magnetic field on the hydrogen evolution activity using non-magnetic Weyl semimetal catalysts. Dalton Transactions 49, 3398–3402.

Hu, F., Jia, Q., Li, Y., Gao, M., 2011. Facile synthesis of ultrasmall PEGylated iron oxide nanoparticles for dual-contrast T1-and T2-weighted magnetic resonance imaging. Nanotechnology 22.

Hu, L., Xia, G., Chen, Q., 2019. Magnetochemistry and chemical synthesis. Chinese Physics B 28.

Hu, L., Zhang, R., Chen, Q., 2014. Synthesis and assembly of nanomaterials under magnetic fields. Nanoscale 6, 14064–14105.

Kolawole, O., Gamadi, T.D., Bullard, D., 2020. Artificial Lift System Applications in Tight Formations: The State of Knowledge. SPE Production & Operations 35, 422–434.

Köne, A.Ç., Büke, T., 2010. Forecasting of CO2 emissions from fuel combustion using trend analysis. Renewable and Sustainable Energy Reviews 14, 2906–2915.

Lashof, D.A., Ahuja, D.R., 1990. Relative contributions of greenhouse gas emissions to global warming. Nature 344, 529–531.

Litvak, S., Litvak, O., 2020. Some Aspects of Reducing Greenhouse Gas Emissions by Using Biofuels. Journal of Ecological Engineering 21, 198–206.

Popescu, M.-A., Isopescu, R., Matei, C., Fagarasan, G., Plesu, V., 2014. Thermal decomposition of calcium carbonate polymorphs precipitated in the presence of ammonia and alkylamines. Advanced Powder Technology 25, 500–507.

Rabczak, S., Proszak-Miąsik, D., 2016. Effect of the type of heat sources on carbon dioxide emissions. Journal of Ecological Engineering 17, 186–191.

Sinharoy, A., Baskaran, D., Pakshirajan, K., 2020. Process integration and artificial neural network modeling of biological sulfate reduction using a carbon monoxide fed gas lift bioreactor. Chemical Engineering Journal 391, 123518.

Song, C., Liu, X., Zheng, H., Bao, C., Teng, L., Da, Y., Jiang, F., Li, C., Li, Y., Xuan, Y., Ding, Y., 2021. Decomposition kinetics of Al- and Fe-doped calcium carbonate particles with improved solar absorbance and cycle stability. Chemical Engineering Journal 406, 126282.

Syed, F.I., Alshamsi, M., Dahaghi, A.K., Neghabhan, S., 2022. Artificial lift system optimization using machine learning applications. Petroleum 8, 219–226.

Useche-Narvaez, C., Montes-Páez, E.G., Guerrero-Martin, C.A., 2022. Evaluation of the carbon footprint produced by conventional artificial lift systems in a Colombian field. Journal of Petroleum Science and Engineering 208, 108865.

Wang, M., Yang, J., 1995. Electrochemical Polymerization of Polyaniline at The Applied Magnetic Field. Synthetic Metals 69, 155–159.

West, T.O., Marland, G., 2002. A synthesis of carbon sequestration, carbon emissions, and net carbon flux in agriculture: comparing tillage practices in the United States. Agriculture, Ecosystems & Environment 91, 217–232.